

AD-A151 365

IN SITU THIN FILM MEASUREMENT(U) ARIZONA UNIV TUCSON  
OPTICAL SCIENCES CENTER H A MACLEOD DEC 84  
AFOSR-TR-85-0081 AFOSR-83-0353

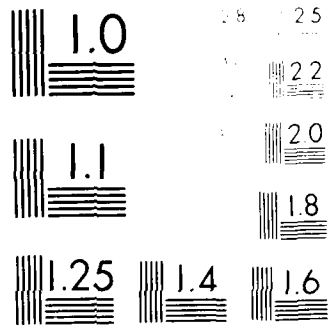
1/1

UNCLASSIFIED

F/G 13/8

NL

						END							
						FILED							
						DTIC							



AFOSR IR

2

CONTRACT NO.  
AFOSR-83-0653

AIR FORCE OFFICE OF SCIENTIFIC RESEARCH  
BOLLING AIR FORCE BASE  
D.C. 20332

AD-A151 365

IN SITU THIN FILM MEASUREMENT

Final Report

H. A. Macleod

Optical sciences Center  
University of Arizona  
Tucson, AZ. 85721



For public release; distribution unlimited.

December 1984

UIC LILL MLL

83 02 18 056

UNCLASSIFIED  
EXEMPT FROM AUTOMATIC  
DECLASSIFICATION

DOCUMENT CONTROL DATA - R & D

REPORT NUMBER: AFOSR-TR-84-010  
TITLE: **UNCLASSIFIED**

PERFORMING ORGANIZATION: **UNCLASSIFIED**

PERFORMING ORGANIZATION REPORT NUMBER: **UNCLASSIFIED**

PERFORMING ORGANIZATION NAME(S) AND ADDRESS(ES): **UNCLASSIFIED**

PERFORMING ORGANIZATION REPORT NUMBER: **UNCLASSIFIED**

A scanning monochromator system for the monitoring and measuring of thin film deposition is described. The system employs data from both a quartz crystal oscillator and a wide band transmission spectrometer. The spectrometer uses a holographic grating as its dispersive element and a CCD array to collect the data. All data is sent to a microcomputer where the information is displayed, stored, and analyzed. Several applications are explored.

DEVELOPMENT OF AN AUTOMATED SCANNING MONOCHROMATOR  
FOR MONITORING THIN FILMS

F.J. van Milligen, Bernhard Goward, Michael R. Jacobson,  
James Mueller, Ross Potoff, Richard L. Shoemaker, H. Angus MacLeod

University of Arizona  
Optical Sciences Center  
Tucson, Arizona 85721

ABSTRACT

A scanning monochromator system for the monitoring of thin film deposition in a box coater is described. The system employs data from both a quartz crystal oscillator and a wide band transmission spectrometer. The spectrometer uses a holographic grating as its dispersive element and a CCD array to collect the data. All data is sent to a microcomputer where the information is displayed, stored, and analyzed. Several applications, including measurement of refractive constants of inhomogeneous films and characterization of moisture adsorption, are discussed.

✓  
PER CALL JR

A-1

APPENDIX I

## Introduction

The objective of this contract was the supporting of a Post-Doctorate Assistant, Dr. Bertrand Bovard, from the Ecole Nationale Supérieure de Physique, Marseille, France, for a stay of one year at Optical Sciences Center to assist in the development of a rapid-scanning spectrometric system for in situ measurements on optical thin films. Dr. Bovard had been awarded his doctorate in Marseille for work on this topic.

## Monochromator

The measuring system was largely constructed with the help of two DARPA contracts, one monitored by NWC, China Lake, and the other by NOSC, San Diego. It consists of a concave holographic grating with a CCD array detector in the spectrum plane. The grating was specifically designed to be used with array detectors and the spectrum plane is flat over the width of the detector. A spectral range from approximately 450 nm to 800 nm is scanned by the system.

Details of the system are described in Appendix 1, the draft of a paper that is being submitted to Applied Optics.

## Thin Film Measurements

Most thin films are inhomogeneous, especially the refracting oxides. Optical inhomogeneity is difficult to measure accurately after deposition. Although the presence of inhomogeneity can readily be detected, the results are insensitive to the specific refractive index profile.

Thus, if we are to have information about the variation of refractive index through the film, additional information (such as in situ measurements made in the coating plane during deposition) are particularly attractive. We must make the assumption of film stability, that is, that the portion of the film already deposited remains unchanged while further material is added. Results that obviously violate this assumption indicate unstable films. We find that well oxidized, regularly deposited titania films are usually stable but that films deposited in the dark with oxygen deficiencies can show unstable behavior.

Further details of the in situ measurement system and of the techniques for analysis are given in Appendices 1 and 2, the texts of two papers that are being submitted to Applied Optics.

## 1. INTRODUCTION

After an optical filter has been satisfactorily designed, it must be implemented in a production facility. For anything but the simplest of multilayer stacks, this involves the selection of the proper process parameters for a specific set of materials in a particular vacuum chamber. The length of time required to control this process fully depends upon the efficiency and fidelity of the monitoring techniques available to the operator. In general, there are two means of monitoring film deposition:

1. Optical monitoring: This technique is more appropriate in realizing coatings consisting of quarterwave layers by detecting the extrema of transmission or reflectance at a particular wavelength. This method is extremely stable for the control wavelength and only slightly less stable around it.<sup>1</sup> Therefore, it is used for coatings designed for performance over a narrow wavelength region.

2. Physical Mass Monitoring: By observing the natural resonance frequency of a quartz crystal, it is possible to determine the mass deposited on its surface; assuming densities for the film materials, one can compute the thickness of the layers. With this technique one can monitor layers of any thickness with high sensitivity. Unfortunately, since it does not include any measurements on the optical performance, it does not provide the stability of optical monitoring, and demands accurate calibration and reliable density data.

In this paper, we will describe a scanning monochromator system which employs both of these techniques in parallel with the added advantage of measuring the optical transmission of the sample over a wide wavelength range. We continue by discussing relevant features of the system and considering some of its applications.

## 2. IMPLEMENTATION

It is appropriate to begin by mentioning that our system was inspired by one built by the group led by Felletier in Marseilles, France.<sup>2,3</sup> Our scanning monochromator system was intended to augment the capabilities of a Balzers 760 box coater, which was delivered with an automated process controller (Balzers Model KB 100) based on a quartz crystal monitor and a second, unautomated, single wavelength optical monitor (Balzers Model 331-210). The front end of the first subsystem was left intact; the second subsystem was replaced with our widened optical monitoring portion of the scanning monochromator system.

Figure 1 is a descriptive flow diagram of the scanning monochromator system. To ensure that the signal reaching the CCD array is adequate, the original Balzers light source was replaced with a tungsten-halogen 100 W tungsten-halogen lamp. This source met the required spectral energy light to saturate the detectors and simultaneously to rely on a single 1000 reference line for wavelength calibration. Unfortunately, the spectral profile shown in Figure 2A, while adequate, and does not extend to the important

ultraviolet region. To solve this problem, we are currently replacing the tungsten-halogen with a xenon arc lamp which will have both a flatter spectrum and output in the ultraviolet, shown in Figure 2B.

Immediately adjacent to the source, the beam is modulated by a four-section chopper, which also provides a reference signal to the lock-in amplifier, part of the detector electronics beyond the detector. After the chopper, the light is projected by a lens into the chamber via a port in the baseplate, through the witness, or reference sample, and back out through a port in the chamber roof. For some experiments, a rotating fixture moves more than one sample through the monitor beam, permitting *in situ* coating comparisons. Figure 3 depicts the overall arrangement of the scanning monochromator with respect to the original box-coater.

After exiting the chamber, the beam is turned by a flat mirror into the main scanning monochromator optics. First, it is re-focused by a lens onto a slit, which is 1 cm high and approximately 0.2 cm wide. After the slit, the beam encounters the dispersive element of the scanning monochromator, a Jobin-Perkin-Elmer gratifyingly perfective grating, ruled at 600 lines/cm and designed to disperse light with a wavelength ranging from 400 to 900 nm, or which we use 440 to 800 nm with a 1000 line/cm grating. The grating is a reflective optical device through which light from the source is directed. Light is directed at the grating at an angle of 45 degrees. The light is dispersed at an angle of 45 degrees. The light is dispersed at an angle of 45 degrees.

each long CCD array matches the one-to-one flat field of the CCD at that point.<sup>4</sup> A view of this part of the monochromator appears in Figure 4.

The CCD array consists of 1728 elements: our signal processing electronics averages sets of ten adjacent elements, providing us with 173 data points. These data levels are sent on to a dedicated IBM-PC, which records the data on five-inch floppy disks and displays them on an amber video monitor for real-time feedback to the plant operator. At the same time, information from the original process controller, based on the quartz crystal monitor, is sent through an interface module to the IBM-PC.

A schematic showing how the computer handles the data appears in Figure 5. The IBM-PC incorporates a Tecmar A/D board, which accepts 12-bit data from both the quartz crystal monitor and the CCD array. Although the electronics are capable of running at a rate of four spectra per second, we generally take one spectrum every three seconds. This is quite adequate, since at our typical deposition rates (primarily oxides), we deposit ten to twenty Angstroms of material in three seconds. The potential for data rates at least an order of magnitude higher would permit us to monitor extremely rapid changes if the need arose. Table 1, below, summarizes important characteristics of the scanning monochromator monitor.

Wavelengths and wave lengths are calculated by identifying a reference point in the light path and then setting a reference wavelength to the diffraction grating. For

readings other than those given by the absorption lines the wavelength is determined by linear interpolation between known points. We estimate an accuracy of 2 to 4 nm over the range we have tested with available spectral line sources.

### 3. APPLICATIONS

Several examples of applications for the scanning monochromator monitor follow:

1) A sequence of transmission spectra for each run can be stored for later analysis of the effects of various process parameters. A 160K double-density 5.25 inch disk can accommodate about 50 minutes of continuously monitored spectral data.

2) The wideband transmission spectra that appear on the monitor provide the plant operator with a much broader view of coating progress; should problems arise, the operators can base their decisions during deposition on a larger data base.

3) Monitoring done in situ permits testing and observation of coatings without removing them from the system. One example of this feature is shown in Figure 5; it examines the effect of water adsorption on a filter.<sup>5</sup>

4) The larger data base available to the computer permits better curve fitting to a film's optical constants. Figure 7 shows the optical constants for a film of  $TiO_2$  as it grows. We note that the computer fits the data very well and, with the use of a list of known wavelengths, the computer can determine the thickness of the coating.

length at a particular thickness. <sup>9</sup>

#### 4. ACKNOWLEDGMENTS

The development of our scanning monochromator system was inspired by a pioneering system constructed at the Laboratoire d'Optique de l'Ecole Nationale Supérieure de Physique de Marseille, France, led by E. Pelletier and including F. Flory, A. Fontier, and H. Richier. One other member of that group is among the authors of this paper; we were fortunate enough to have B. Bovart as a post-doctoral scientist for one year at the Optical Sciences Center. His visit had an extremely stimulating influence on the construction and completion of the instrument. The Air Force Office of Scientific Research (AFOSR) provided salary support for his year in Arizona. We would also like to thank T. G. Ferguson and Russell Chipman of the Optical Sciences Center for their helpful discussions. M. DeGood skillfully executed the figures. We also would like to thank the Defense Advanced Research Projects Agency (DARPA) for their generous support of our fiber optics research through a three-year contract maintained by the Optical Sciences Center.

2. REFERENCES

1. H.H. MacLeod, "Tuning-Value Monitoring of Narrow-Band Antireflection Thin Film Optical Filters," *Optical Engng.*, **19**, 1963, p. 1072.
2. R. Esvolder and E. Pelletier, "Optical Thin Film Monitoring - Recent Advances and Limitations," *Thin Solid Films*, **77**, 1969, p. 149.
3. R. Esvolder, R. Fournier, and E. Pelletier, "Wideband Optical Monitoring of Narrow-Band Inter-Layer Multilayer Filters," *Applied Optics*, **18**, 1979, pp. 173-174.
4. G.M. Lerner, D. F. Shepard, J.R. Lytle, G. Pastorek, and A. G. Fox, "Intermittent Drawings Filtered and Holographic - A Review," *IBM J. Res. Develop.*, **19**, 1975, p. 249.
5. R. Esvolder, G. Meunier, R. Esvolder, L. Desjardins, R. D. Van Der Weert, and H.W. Marwick, "Ion Bombardment-Induced Retarded Growth of Antireflection Coatings on Thin Films," *Applied Optics*, **23**, 1984, p. 1072.
6. R. Esvolder, G. Meunier, G. Pastorek, R. D. Van Der Weert, and H.W. Marwick, "Ion Bombardment-Induced Retarded Growth of Antireflection Coatings on Thin Films," *Applied Optics*, **23**, 1984, p. 1072.
7. R. Esvolder, G. Meunier, G. Pastorek, R. D. Van Der Weert, and H.W. Marwick, "Ion Bombardment-Induced Retarded Growth of Antireflection Coatings on Thin Films," *Applied Optics*, **23**, 1984, p. 1072.
8. R. Esvolder, G. Meunier, G. Pastorek, R. D. Van Der Weert, and H.W. Marwick, "Ion Bombardment-Induced Retarded Growth of Antireflection Coatings on Thin Films," *Applied Optics*, **23**, 1984, p. 1072.

A nonabsorbing inhomogeneous layer, provided it is reasonably thick and there is appreciable index contrast at its boundaries, can be represented by the characteristic matrix<sup>21</sup>

$$\begin{bmatrix} \cos \delta & i \sin \delta (n_{\text{out}}/n_{\text{in}})^{1/2} \\ i \sin \delta (n_{\text{out}}/n_{\text{in}})^{1/2} & \cos \delta \end{bmatrix} \quad (8)$$

where  $n_{\text{out}}$  is the index at the outer surface of the film

$n_{\text{in}}$  is the index at the inner surface of the film, and

$\delta$  is the phase thickness.

If we assume that the absorption is very small, the same matrix can be

used with the extinction coefficient included in  $\delta$  only so that

$$\delta = \bar{n}d + i\bar{k}d$$

where  $\bar{n}$  is the mean index of the film (i.e.  $\bar{n} = \frac{1}{d} \int_0^d n(z)dz$ ),

$\bar{k}$  is the mean extinction coefficient (i.e.  $\bar{k} = \frac{1}{d} \int_0^d k(z)dz$ ),

$d$  is the thickness, and

$i$  is the imaginary unit of the layer.

It is assumed that the incident medium has a refractive index  $n_0$  and

the substrate has a refractive index  $n_s$ . After some tedious

algebra we obtain the expression for the transmission of the coated

In the case of negligible extinction coefficients the derivation of the refractive index can be achieved using an admittance circle method based on transmission measurements during the growth of the layer<sup>5</sup>. But since our interests lie more in slightly absorbant materials such as oxides, we have developed a technique inspired by the envelope method described by Manifacier et al (6). We have used an inhomogeneous model of a thin film to derive the refractive index and the extinction coefficient profiles.

#### 3.1.1. Envelope method in the inhomogeneous case

Manifacier et al<sup>6</sup> have fully described the envelope method in the limiting case of an homogeneous thin film where only transmission measurements are required for the derivation of  $n$  and  $k$ . A generalization to an inhomogeneous model was presented by Arndt et al<sup>7</sup> to derive the optical constants from measurements of reflectance and transmittance. In these studies reflection and transmission are considered as functions of wavelength and their envelopes are used to calculate the optical constants. To obtain the profiles of the optical constants, as in this study, we considered the envelopes of the curve of transmittance as functions of thickness for a chosen wavelength. We were able to obtain the dispersion by applying the same method to a range of wavelengths.

We will demonstrate the principle of the method and give the analytical relations for the optical constants.

## I. Introduction

The refractive index and the extinction coefficient of a thin film depend upon the conditions of deposition and as a consequence upon the structure of the film itself. In the case of oxides, inhomogeneities are largely due to the film's columnar structure<sup>1</sup> and to the variations in degree of oxidation throughout the layer. The derivation of their profiles as a function of thickness is difficult once the layer has been deposited. Furthermore, most techniques developed to measure the refractive index are carried out under atmospheric conditions. Exposure of a film to the air modifies its optical properties: the voids existing in its structure tend to adsorb moisture and an oxidation process may occur for a suboxidized layer, changing the refractive index and the extinction coefficient.<sup>2,3</sup> Therefore a technique taking into account the evolution of the transmission of a layer growing in vacuo has great advantages. To achieve such measurements we have used a scanning monochromator system<sup>4</sup> which provides us with the transmission over the visible spectrum versus time, during deposition. Using these values we have developed a technique for deriving the profiles of the optical constants. After a verification of the optical constants determination technique by computer simulation, we have applied the method to various layers of titanium dioxide. This technique can then be used as a means of monitoring the effect on the optical constants of a change in any of the parameters used for the coating process.

II. Determination of the profile of the optical constants of an  
inhomogeneous film

Optical Constants derivation for an inhomogeneous  
thin film from in situ transmission measurements

B. Bovard, F.J. Van Milligen, M.J. Messerly, S.G. Saxe, H.A. Macleod

University of Arizona  
Optical Sciences Center  
Tucson, Arizona 85721

ABSTRACT

The optical constants of a thin film depend upon the structure of the film itself. A technique, based on transmission measurements carried out in vacuo, has been developed to derive the profiles of the refractive index and extinction coefficient. The interpretation of the profiles gives information on the layer structure in vacuo. The technique can be used as a means of monitoring the variations of the optical constants with changes in the deposition parameters. This paper presents the technique, which is based on an envelope method, and gives some experimental results.

APPENDIX 2

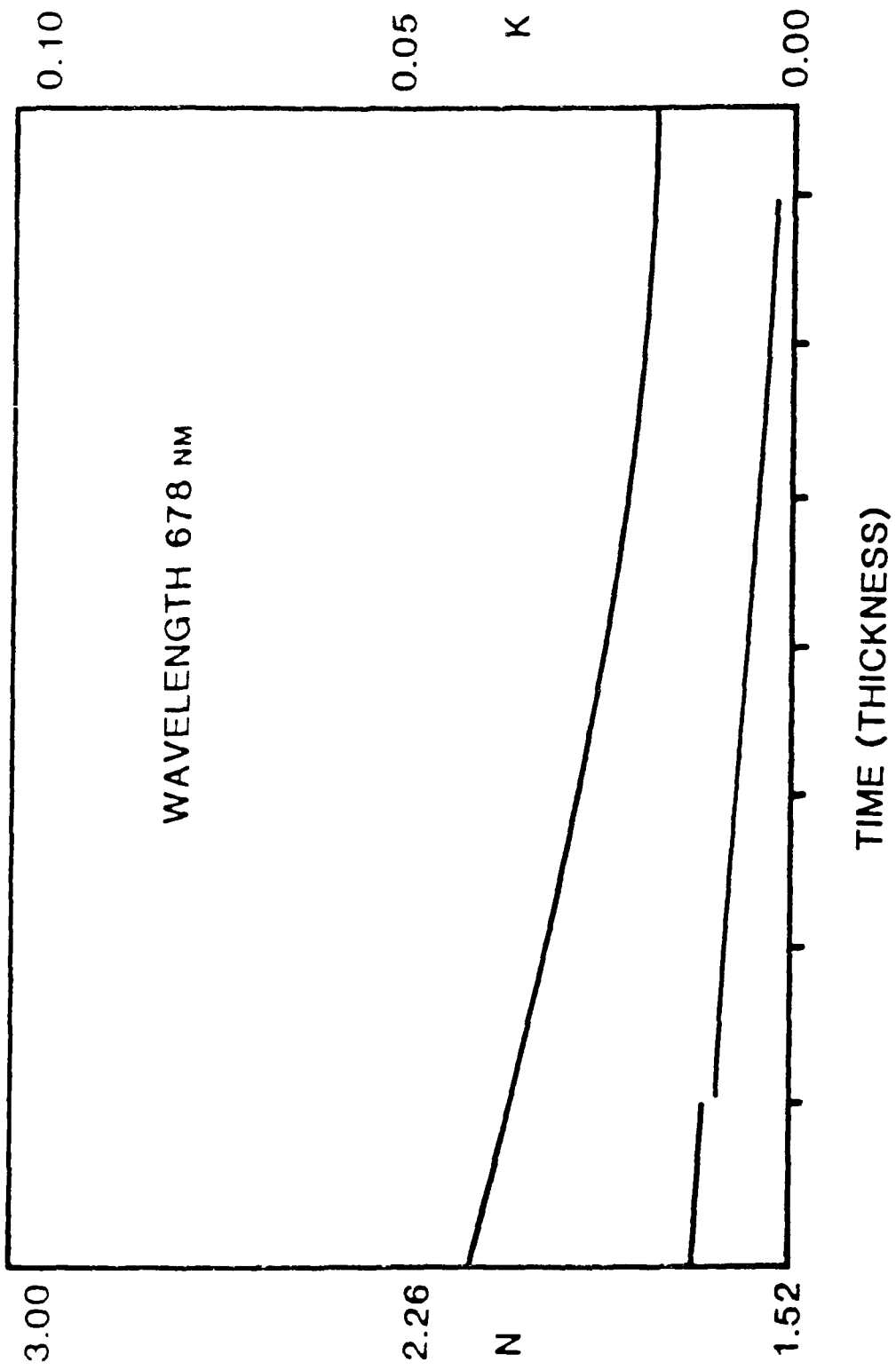


Fig. 7. Variation of optical constants of TiO<sub>2</sub> film as the film is being deposited. Upper curve corresponds to n, lower curve to k.

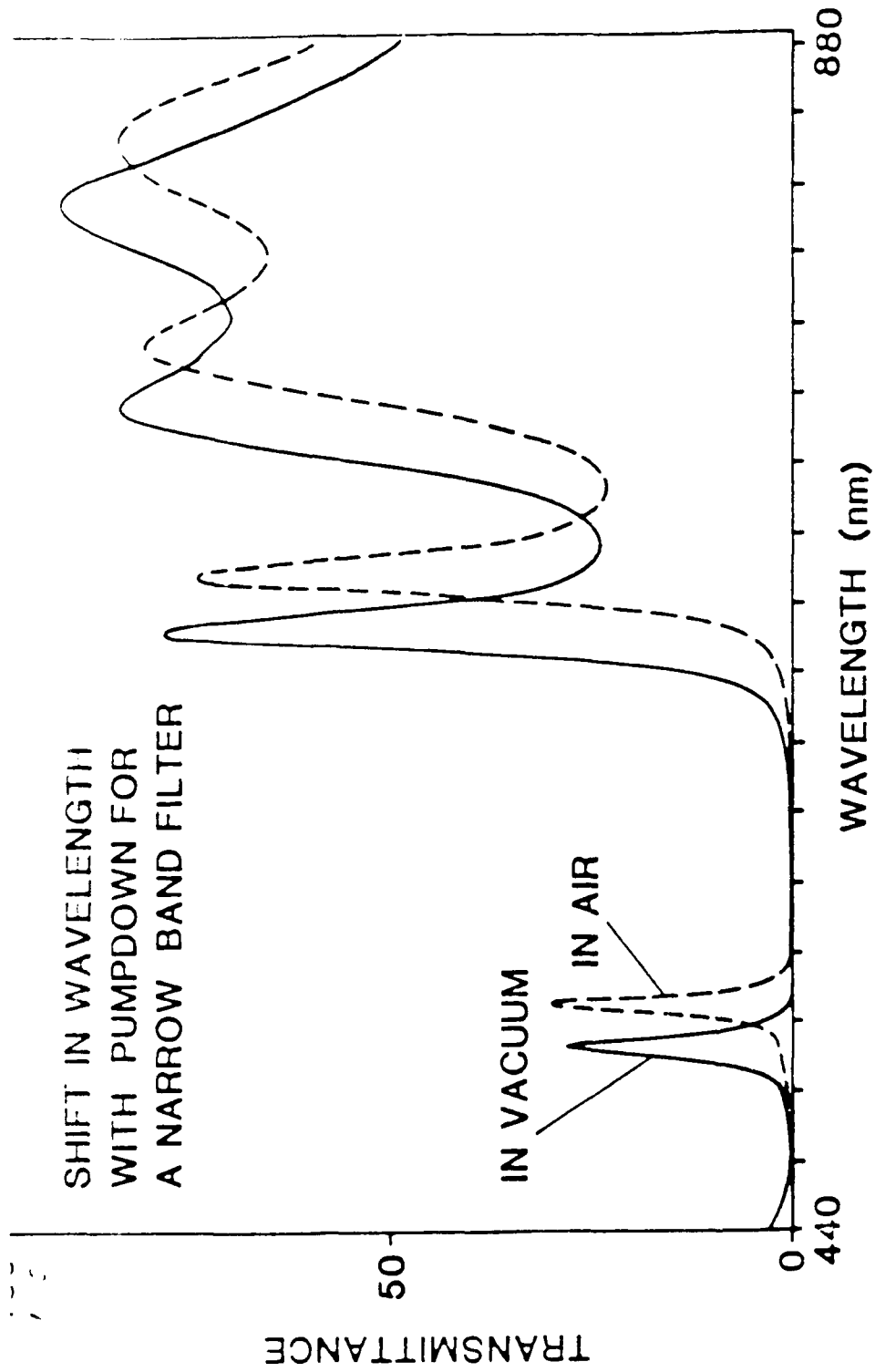


Fig. 6. Example of Water Adsorption in a  $\text{TiO}_2/\text{SiO}_2$  Fabry-Perot Filter

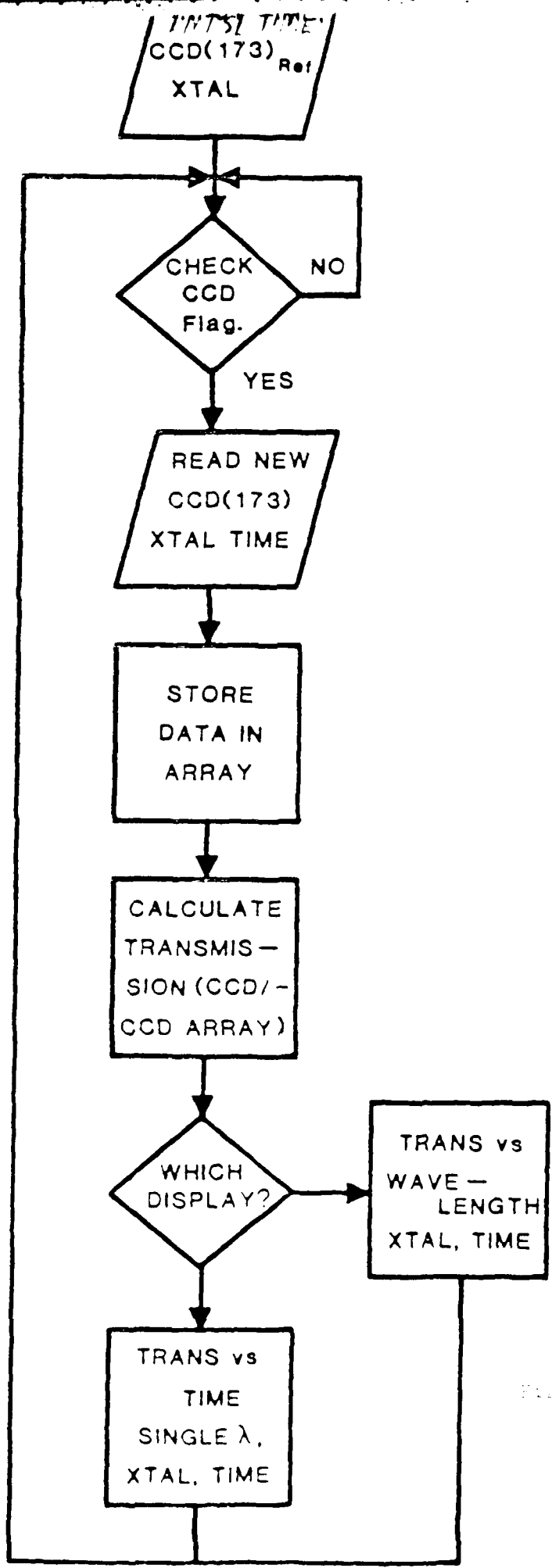
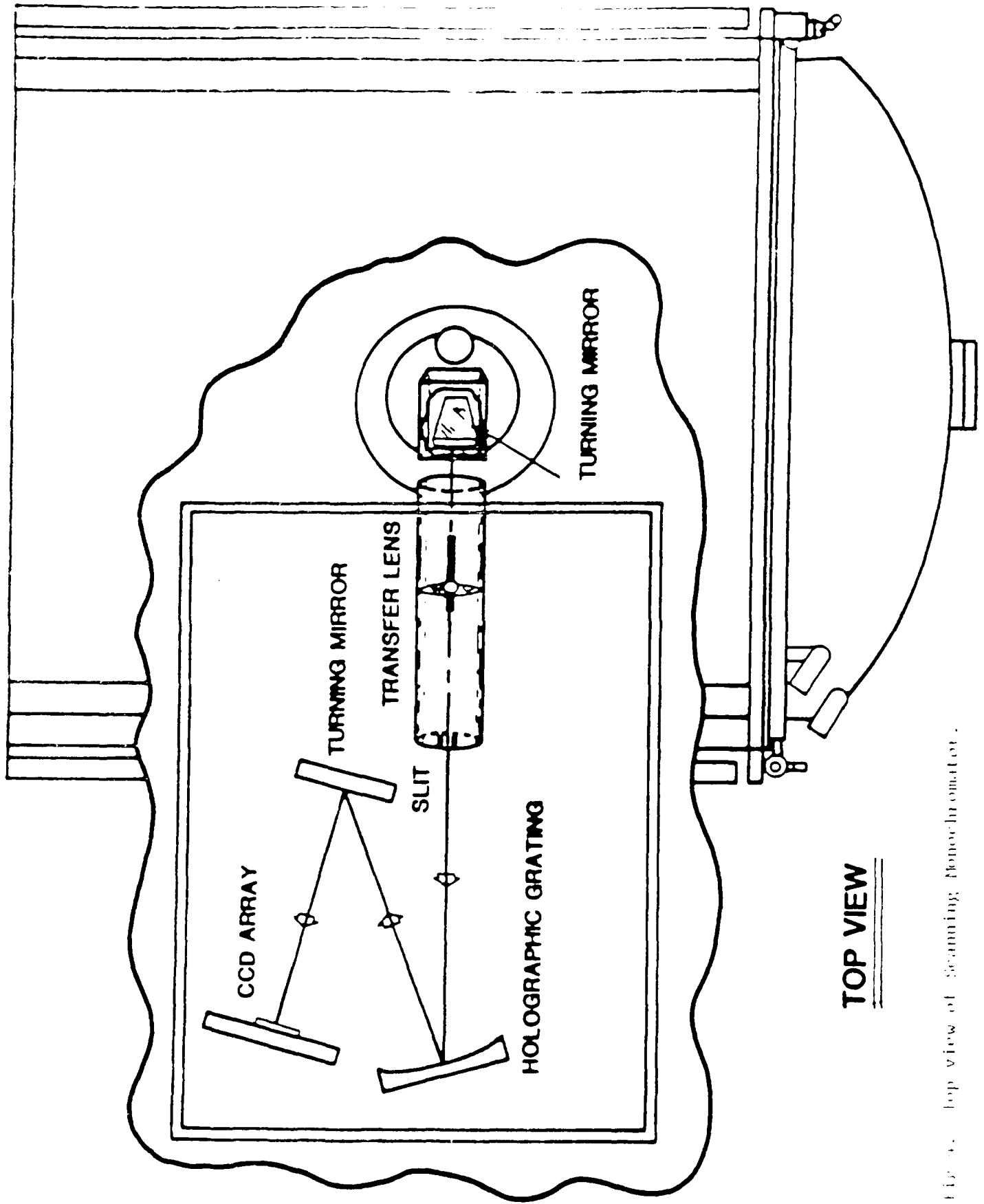


Fig. 1. Flowchart of computer program for handling data.



**TOP VIEW**

Fig. 4. Top view of Scanning Monochromator.

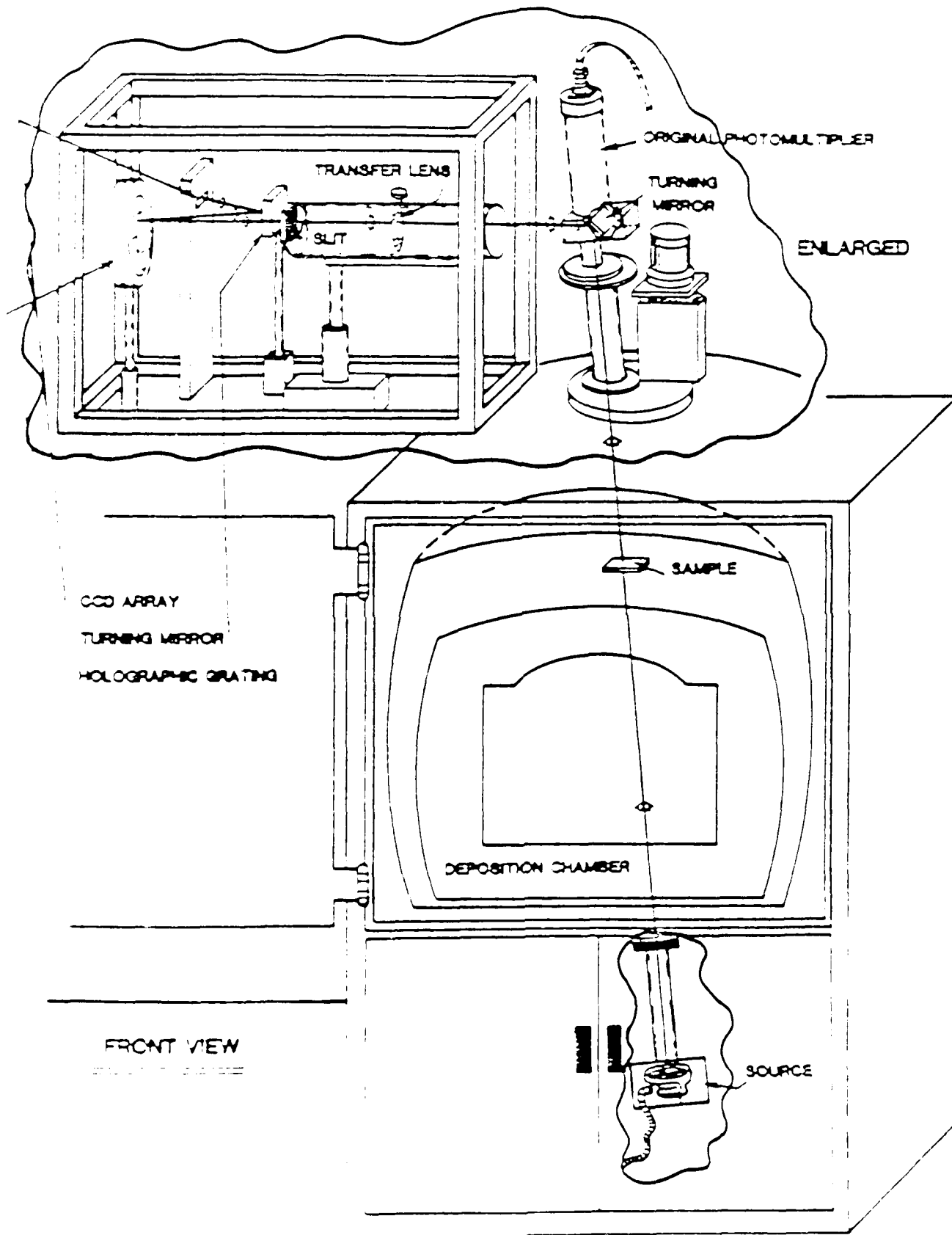


Diagram of the laser-based deposition system.

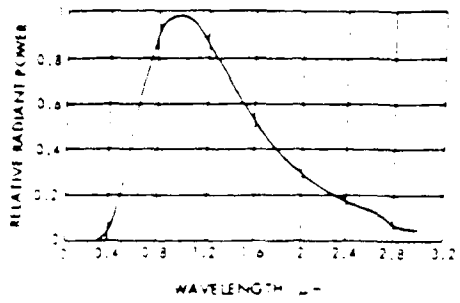


Fig. 14. Spectral Profile of Tungsten Halogen Lamp.

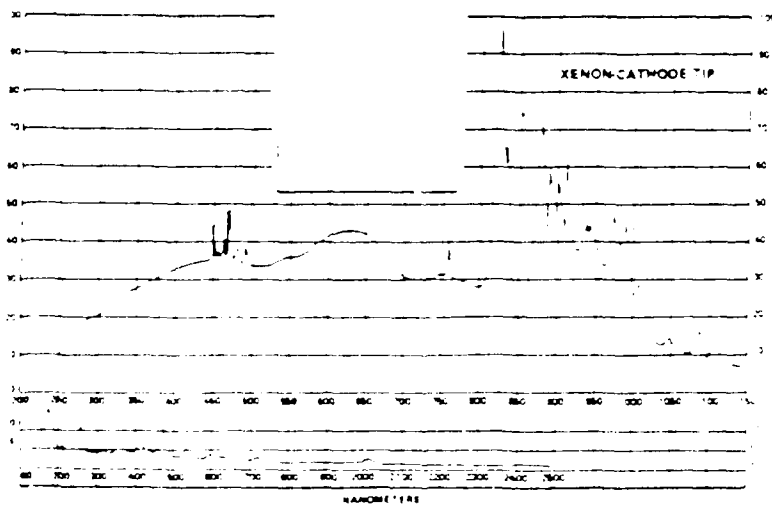


Fig. 15. Spectral Profile of Xenon-Cathode Tip Lamp.

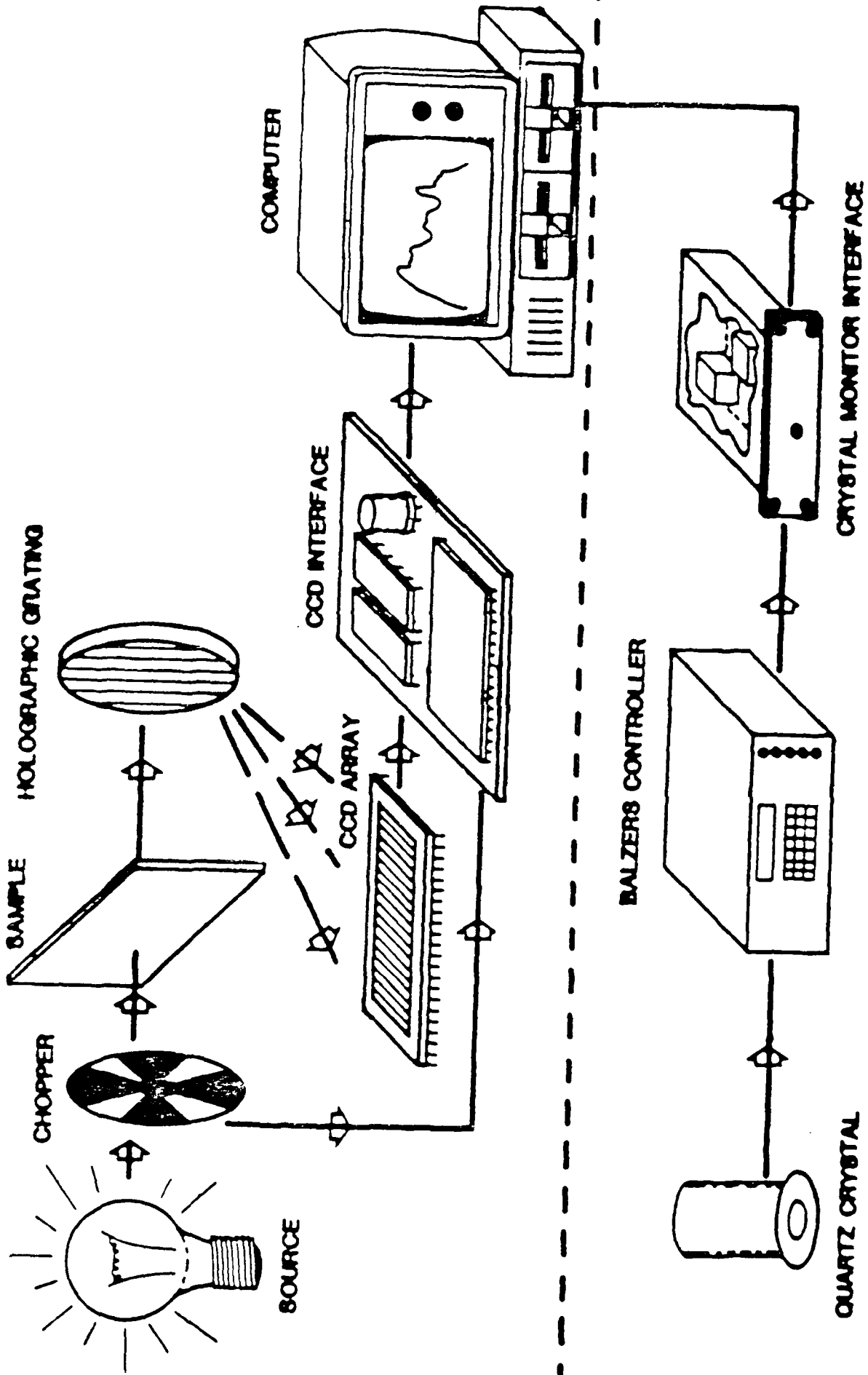


Fig. 1. Scanning Monochromator Flow Diagram.

## FIGURE CAPTIONS

1. Scanning Monochromator Flow Diagram
- 2a. Spectral Profile of Tungsten Halogen Lamp
- 2b. Spectral Profile of Xenon Arc Lamp
3. Appearance of Scanning Monochromator system
4. Top view of Scanning Monochromator
5. Flowchart of Computer Data Handling Program
6. Example of Water Adsorption in a  $\text{TiO}_2$ ,  $\text{SiO}_2$  Fabry-Perot Filter
7. Variation of optical constants of  $\text{TiO}_2$  as the film is being deposited. Upper curve corresponds to  $n$ , lower curve to  $k$ .

TABLE 1: SYSTEM PERFORMANCE

Wavelength Range	440 - 680 nm
Wavelength Resolution	2 nm
Resolving Power	300
Etendue of System	$1 \times 10^{-3} \text{ cm}^2\text{-sr}$
Minimum Transmission	2%
Signal Level of DDD	70% of saturation at 650 nm

$$T = \frac{16n_s n_o n_{in} n_{out} e^{2\delta_1}}{C_1^2 + C_2^2 e^{4\delta_1} + 2C_1 C_2 e^{2\delta_1} \cos 2\delta_1}$$

where  $C_1 = (n_{out} + n_o)(n_s + n_{in})$        $C_2 = (n_{out} - n_o)(n_s - n_{in})$

$$\delta_1 = 2\pi n d / \lambda$$

$$\delta_2 = -2\pi k d / \lambda$$

In the following we shall assume that we are dealing with a high index layer so that  $C_1$  is negative. Then the two expressions of the envelopes become:

$$T_{max} = \frac{16n_o n_s n_{in} n_{out} e^{2\delta_1}}{(C_1 + C_2 e^{2\delta_1})^2}$$

$$T_{min} = \frac{16n_o n_s n_{in} n_{out} e^{2\delta_1}}{(C_1 - C_2 e^{2\delta_1})^2}$$

These two equations are used to determine the outermost index for each instant during film deposition. They are also used to calculate the extinction coefficient at the quarterwave points.

However, all these derivations are possible only if we make a very basic assumption about the stability of the layer during deposition. This assumption is simply that the innermost index does not vary during the growth of the film. The profiles of the optical constants can then be derived and considered as functions of thickness instead of time.

We shall not go through the details of the derivation and we shall only give the analytical expressions for the innermost and outermost

refractive index, the geometrical thicknesses and the extinction coefficient profile.

The expression of the innermost refractive index is obtained assuming  $n_{in} = n_{out}$  and  $d = 0$  so that:

$$n_{in} = [N + (N^2 - n_o^2 n_s^2)^{1/2}]^{1/2} \text{ where } N = \frac{n_o^2 + n_s^2}{2} + 2n_o n_s \left( \frac{T_{max} - T_{min}}{T_{max} + T_{min}} \right)$$

The expression of the outermost refractive index is then:

$$n_{out} = \frac{2n_{in} n_s n_o}{n_{in}^2 - n_s^2} \frac{T_{max} - T_{min}}{T_{max} + T_{min}} + n_o \left[ 1 + 4n_{in}^2 n_s^2 \left( \frac{T_{max} - T_{min}}{T_{max} + T_{min}} \right)^2 / (n_{in}^2 - n_s^2)^2 \right]^{1/2}$$

which is calculable only if we know the innermost index value.

Provided we assume the innermost index is stable we can calculate the profile of the refractive index of an inhomogeneous layer. Note that it requires the knowledge of the substrate refractive index, which can be measured independently, but it does not require the value of wavelength.

We also require the geometrical thickness. Since we are dealing with low-absorption materials, the extrema of transmission occur when the optical thickness of the layer is a multiple of a quarterwave.

If  $m$  is the order of the extremum ( $m=1$  indicating the first minimum) the corresponding geometrical thickness is

$$d = \frac{m \lambda}{4 \bar{n}} \text{ where } \bar{n} = \frac{1}{d} \int_0^d n(z) dz$$

since calculation of  $\frac{1}{d} \int_0^d n(z) dz$  is impossible, we make an

approximation and write that  $\bar{n} = \frac{1}{t} \int_0^t n(u) du$  where  $t$  is the instant

when the extremum occurs.

This is equivalent to assuming that the rate of deposition (change in thickness per unit time) is constant. The assumption is reasonable because our deposition rate is automatically controlled.

With regard to the profile of extinction coefficient we note first that a mean value of the extinction coefficient can be derived each time we reach a new quarterwave:

$$\bar{\kappa} = -\frac{\lambda}{4\pi d} \text{Log } a(d) \text{ with } a(d) = \frac{C_1[1-(T_{\max}/T_{\min})^{1/2}]}{C_2[1+(T_{\max}/T_{\min})^{1/2}]} = \exp\left(-4\pi \frac{\bar{\kappa}d}{\lambda}\right)$$

but since the function  $a$  is available at any instant during the growth of the layer, we can also calculate its derivative versus time and obtain an expression giving the profile of extinction coefficient.

$$\kappa(z) = -\frac{\lambda}{4\pi} \frac{1}{a(z)} \frac{da}{dz} \text{ where } z \text{ is the thickness of the layer.}$$

Because of the derivative, this expression presents some sensitivity to errors but can still be used to obtain an indication of the absorption of the material.

## 11.2. Stability of deposition and conclusion

Provided we know the envelopes of a curve of transmission, using these analytical expressions we are able to derive the optical constants. But the necessity of knowing the envelopes as functions of thickness leads us to a very basic assumption concerning the stability of growth of the layer. The envelopes calculated using the measured transmission versus time are usable if they do not shift during the deposition process, which means that an earlier part of the layer is not modified during the deposition of a later part.

It is easy to foresee the importance of having an accurate way of determining extrema of the transmission curves. Their precise estimation, both value and position, demanded that we consider some numerical treatments of the raw data before calculating the envelopes fitting these points. We present in the next section the data processing techniques developed together with a justification of their validity and of the expressions presented above.

### III. Data Processing and Simulation

The envelope computation requires an accurate knowledge of the data points together with a method to fit curves to these points. It was thought possible that the data processing used for the computation of the envelopes might introduce a bias in the results given by the program of optical constant determination. However, we are able to show that this was not the case so that our results are free from such effects.

#### III. 1. Smoothing the curve of transmission versus time

Many methods are available for smoothing, but our requirement was to smooth without distorting the curve. For this reason we decided to use a filtering method based on a finite impulse response filter designed to have a linear phase and an extremely flat low-pass band. We thus avoid any distortion introduced by a nonlinear phase and the attenuation due to a nonflat passband. The filter does still introduce a delay equal to the derivative of its phase versus frequency, but this delay is constant and is corrected in the computation by an entire shift of the curve. Details of this type of approach are given in (9) which inspired the present design and so we limit our description to demonstrating its application to a real signal in Figs. 1 and 2.

#### III. 2. Envelope computation

The ordinates of the envelopes are computed by segments. The first segment of three points gives a parabola which is used to describe the curve between the first two points. Next the first point is discarded and replaced by the fourth point. A new parabola is now

calculated and used to describe the segment between the second and third points. This operation is repeated until the entire curve is produced.

### III. a. Verification and precision of the technique

The validity of the expressions for the refractive indices and the extinction coefficient has been checked by some simulations, the results of which are presented here.

A program able to handle variable optical constants has been developed to compute the evolution of the transmission of a coated substrate during growth of a thin film. The profiles of the optical constants are fed into the program which divides the inhomogeneous layer into a stack of homogeneous sublayers each of thickness  $1\text{nm}$ . The transmittance is then recorded on disk files exactly as when the scanning monochromator is used. The optical constant determination program is then used to compute the index and extinction coefficient profiles. Their comparison with the original ones verifies the accuracy of the technique. Our goal was also to show it is possible to separate the inhomogeneity of the refractive index from the extinction coefficient. Of the many computations that have been performed we simply show two of the most characteristic ones.

The simplest case is that of a homogeneous layer. Taking starting values of  $n = 1.3$  and  $k = 10^{-4}$ , the optical constants were calculated for two wavelengths 400 and 800 nm and the indices found were to be 40% lower than the initial value. As foreseen, the efficiency of the

Simulation of the extinction coefficient was not as good, leading to a 1.5% relative error.

To test the derivation in the case on an inhomogeneous layer, an arbitrary curve of refractive index was chosen to compute the evolution of transmission :  $n(d) = 2 + 0.3 \exp(-d/200)$  where  $d$  is the thickness of the layer. The extinction coefficient was assumed constant equal to  $0.01$ . Table 1 shows the calculated results for two wavelengths. The columns  $\Delta n_{in}$ ,  $n_{in}$  etc. list the error in the determination expressed as a percentage.

TABLE 1

Wavelength (nm)	$n_{in}$	$\Delta n_{in}/n_{in}$	$n_{out}$	$\Delta n_{out}/n_{out}$	$\kappa$	$\Delta \kappa/\kappa$
400	2.297	0.15%	2.012	0.09%	$1.03 \times 10^{-3}$	7%
800	2.283	1%	2.025	0.7%	$0-1.7 \times 10^{-3}$	-

Results of simulation calculations

These results indicate that we can expect acceptable accuracy in the refractive index profile using this technique. It is important to note that the higher accuracy corresponds to the shorter wavelength. This is due to the greater number of extrema at the shorter wavelength, which provides more information so the envelopes calculated have a more exact position. This inaccuracy of the envelopes leads to questionable values of the extinction coefficient for the longer wavelength. These results are rigorously true only for the cases considered but they strongly suggest what we can generally expect from this method. The relative accuracy of the refractive index depends also upon the quality of the transmittance measurements: it ranges from  $\Delta T/T$  to  $5\Delta T/T$  where  $\Delta T/T$  is the relative accuracy achieved in the transmittance measurements.

#### IV. Experimental results

The optical constant determination has been carried out for titanium dioxide layers only. We will present the results obtained with two different layers, the first layer fitting the model used in this derivation and the second being unstable.

The starting material used in our experiments was  $Ti_2O_3$ , evaporated by electron bombardment onto a glass substrate.

For the first layer we consider, the oxygen partial pressure was  $4 \times 10^{-7}$  mbar and the chamber temperature varied from  $204^\circ$  to  $227^\circ C$  during the deposition.

The profile of refractive index and of extinction coefficient are plotted in Fig. 3 for the wavelength 678 nm. The thickness of the layer is 670 nm, the inner index is 2.135 and the outermost index 1.794. The layer is inhomogeneous, as expected for an oxide layer, and slightly absorbant.

The correlation between index and extinction coefficient can be interpreted as an increase of the degree of oxidation with the thickness of the layer and as a decrease of the packing density due to a conical form of the columnar structure. It is difficult to choose which has the primary effect.

Fig. 4 gives the dispersion of the innermost and outermost refractive indices. A high dispersion for the outermost index suggests a more absorbant outer part of the layer.

The layer appears to be stable and therefore our results indicate that it is an inhomogeneous layer showing a decrease in its packing density and a decrease in its oxidation degree in the direction of growth.

We now examine an unstable layer. This layer was deposited in a chamber at a temperature of 250°C in the presence of oxygen at a partial pressure of  $1.1 \cdot 10^{-7}$  mbar.

This atmosphere was intentionally deficient in oxygen compared with the usual conditions for the deposition of titanium dioxide and we expected some absorption in the layer. We are not disappointed as shown Fig. 5

but furthermore another phenomenon seems to occur. The curve of the extinction coefficient falls with thickness towards a value which could even become negative. This is almost certainly the effect of instability in the oxidation of the layer: starting with a high deficiency of oxygen the inner part of the film is gradually oxidized as the layer grows. This defeats the technique presented here since the extrema used to calculate the envelopes are changing with the oxidation of the layer and also because we have assumed the innermost refractive index to be constant. The real curve is impossible to obtain but we can expect that it would present a less inhomogeneous profile.

Other experiments have been carried out to understand the limitations of this method. The instability of the layer can manifest itself by the appearance of negative extinction coefficients, by thicknesses varying with wavelength or by very misshapen profiles of index. Nevertheless, the application of this technique to stable layers gives very interesting results. These can give information on the structure of the layer in terms of packing density as well as in terms of degree of oxidation. It is also important to know that layers can be unstable and to be able to recognise such an instability. Further work is required in this area. We hope that eventually it may be possible to distinguish an instability caused by a structural rearrangement from a reoxidation of some innermost portions of the film.

## V. Conclusion

This method has been developed for layers presenting a high index, a small homogeneity, and a small extinction coefficient. It permits the determination of the profiles of the optical constants and the dispersion of index in vacuo provided the assumption of stability is fulfilled. It identifies layers that are unstable. It makes possible the study of the variations of the optical constants with changes in the deposition parameters.

Major support for this work was provided by the Defense Advanced Research Projects Agency (DARPA) through a contract with the Naval Weapons Center, China Lake. Additional support was also given by DARPA through a contract with the Naval Ocean Systems Center, San Diego. Bovari was supported by the Air Force Office of Scientific Research and Saxe by a fellowship from the U.S. Army Research Office.

References

1. H.A. Macleod. "Microstructure of optical thin films." Proc SPIE 45 pp11-18 (1982).
2. Cheng-Chung Lee. "Moisture adsorption and optical instability in thin film coatings." Ph.D. dissertation, University of Arizona (1983).
3. J. P. Borgogno, P. Bousquet, F. Flory, B. Lazarides, E. Pelletier and P. Roche. "Inhomogeneities in films: limitation of the accuracy of optical monitoring of thin films." Applied Optics 20 pp90-94 (1981).
4. F. Van Milligen, B. Bovard, M.R. Jacobson, J. Mueller, R. Potoff, H.A. Macleod, R. Shoemaker, University of Arizona. "Development of an Automated Scanning Monochromator for a Balzers 760 Evaporation System." Paper presented at OSA Annual Meeting, San Diego, October 1984.
5. Schmitt, Thèse de docteur ingénieur "Problèmes de réalisation des filtres spectraux multidiélectriques: contrôle simultané de l'indice de réfraction et de l'épaisseur des couches en cours de formation." Ecole Nationale Supérieure de Physique, Marseille (1983).
6. M. Maittner, J. Gaslot, J.P. Fillard. "A Simple method for the determination of the optical constants  $n$ ,  $k$  and the thickness of a weakly absorbing thin film." Journal of Physics E: Scientific Instruments, 9 pp101-4 (1976).
7. J.P. Arndt, R.M.A. Azzam, J.M. Bennett, J.P. Borgogno, D.K. Cheng, W.W. Case, M.A. Dobrowolski, G.D. Hobson, I. Tittleman,

Forrest, V.A. Hodgkin, W.P. Klapp, G.A. Macleod, E. Pelletier, M.K. Purvis, D.M. Quinn, D.H. Strome, R. Swenson, P.A. Temple, T.F. Thoun. "Multiple Determination of the Optical Constants of Thin Film Coating Materials." Applied Optics, 23 pp3571-3596 (1984)

3. K. Jacobsson. "Inhomogeneous and coevaporated homogeneous films for optical Applications." Physics of Thin Films, ed. G. Hass, M.H. Francombe and R.W. Hoffman, 3 pp51-98 Academic Press (1975).

4. S.M. Bozin. "Digital and Kalman Filtering. An Introduction to Discrete Time Filtering and Optimum Linear Estimation." Edward Arnold, London (1979).

## FIGURE CAPTIONS

1. Plot of noisy signal. The extrema are difficult to determine with accuracy.
2. After filtering, the extrema have been extracted from the noise without distorting or attenuating the transmission curve.
3. Profile of refractive index and extinction coefficient for a stable titanium dioxide layer. (Upper curve represents  $n$ , lower curve  $k$ ).
4. Dispersion of innermost and outermost refractive index for a stable layer of titanium dioxide.
5. Example of result given by the method when applied to an unstable layer. Titanium dioxide layer deposited in an oxygen deficient atmosphere.

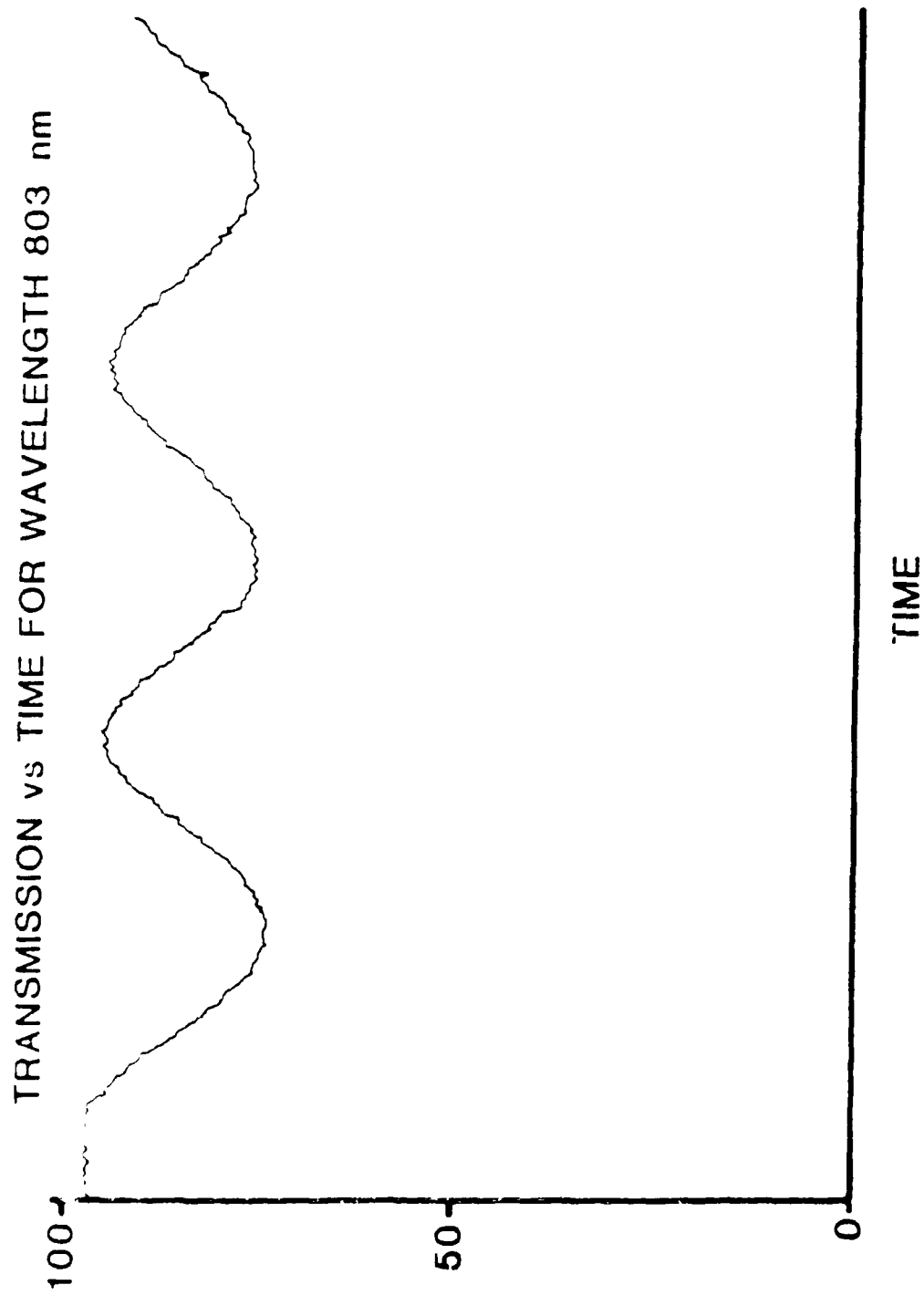


Fig 1. Plot of noisy signal. The extrema are difficult to determine with accuracy.

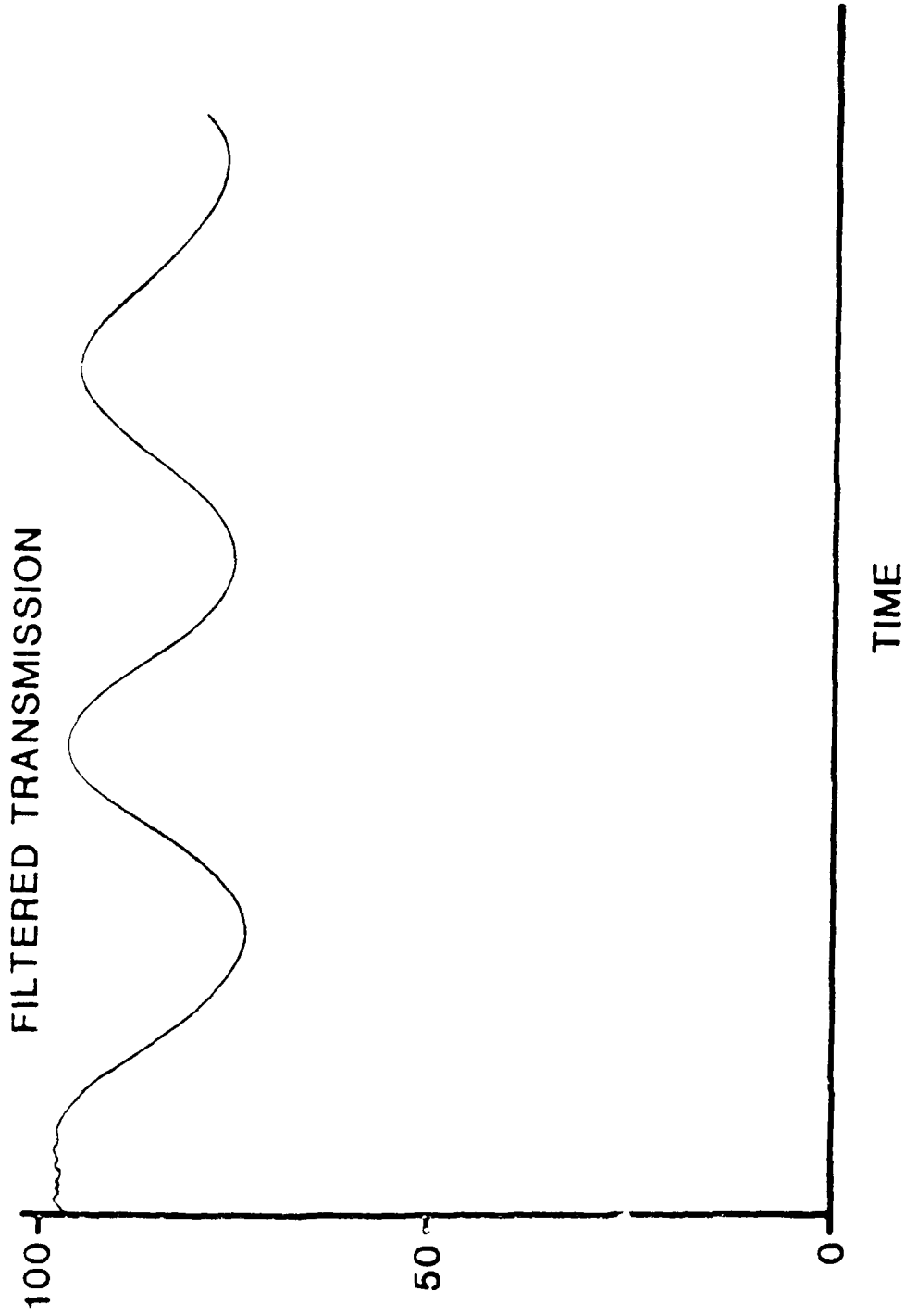


FIG. 2. After filtering, the extrema have been extracted from the noise without distorting or attenuating the transmission curve.

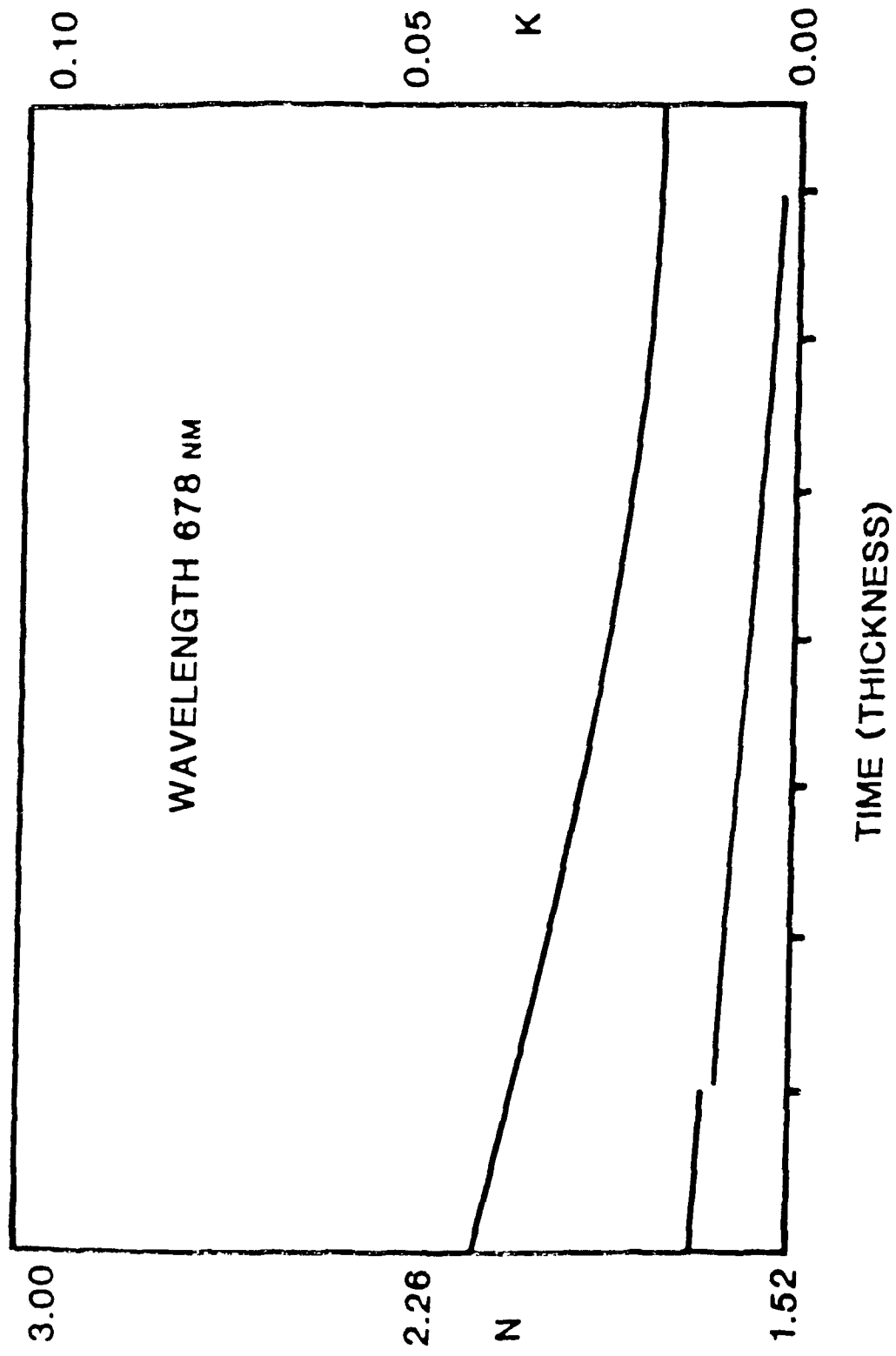


FIG. 3. Profile of refractive index and extinction coefficient for a stable Titanium Dioxide layer. (Upper curve represents n, lower curve k).

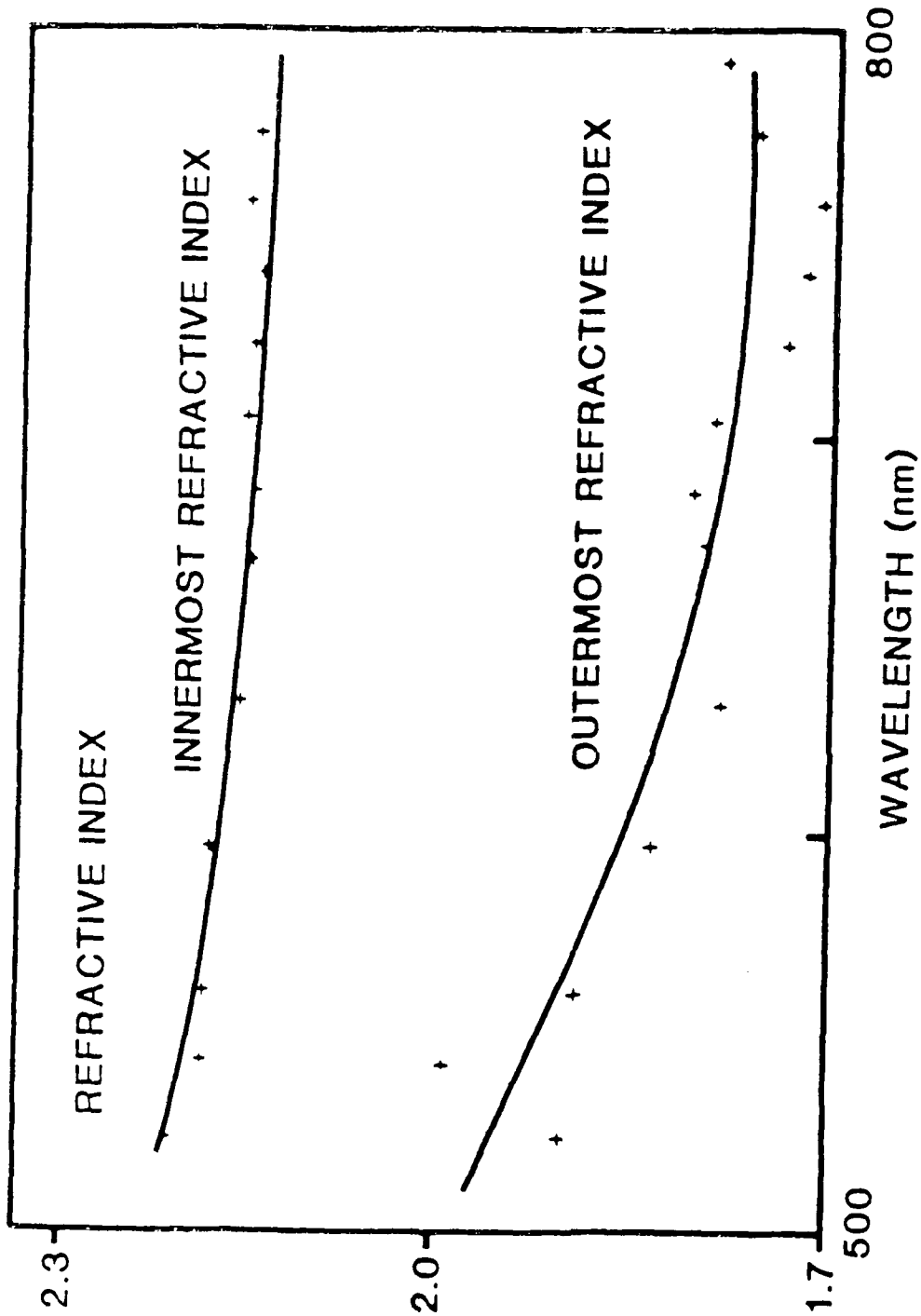


FIG. 4. Dispersion of innermost and outermost refractive index for a stable layer of titanium dioxide.

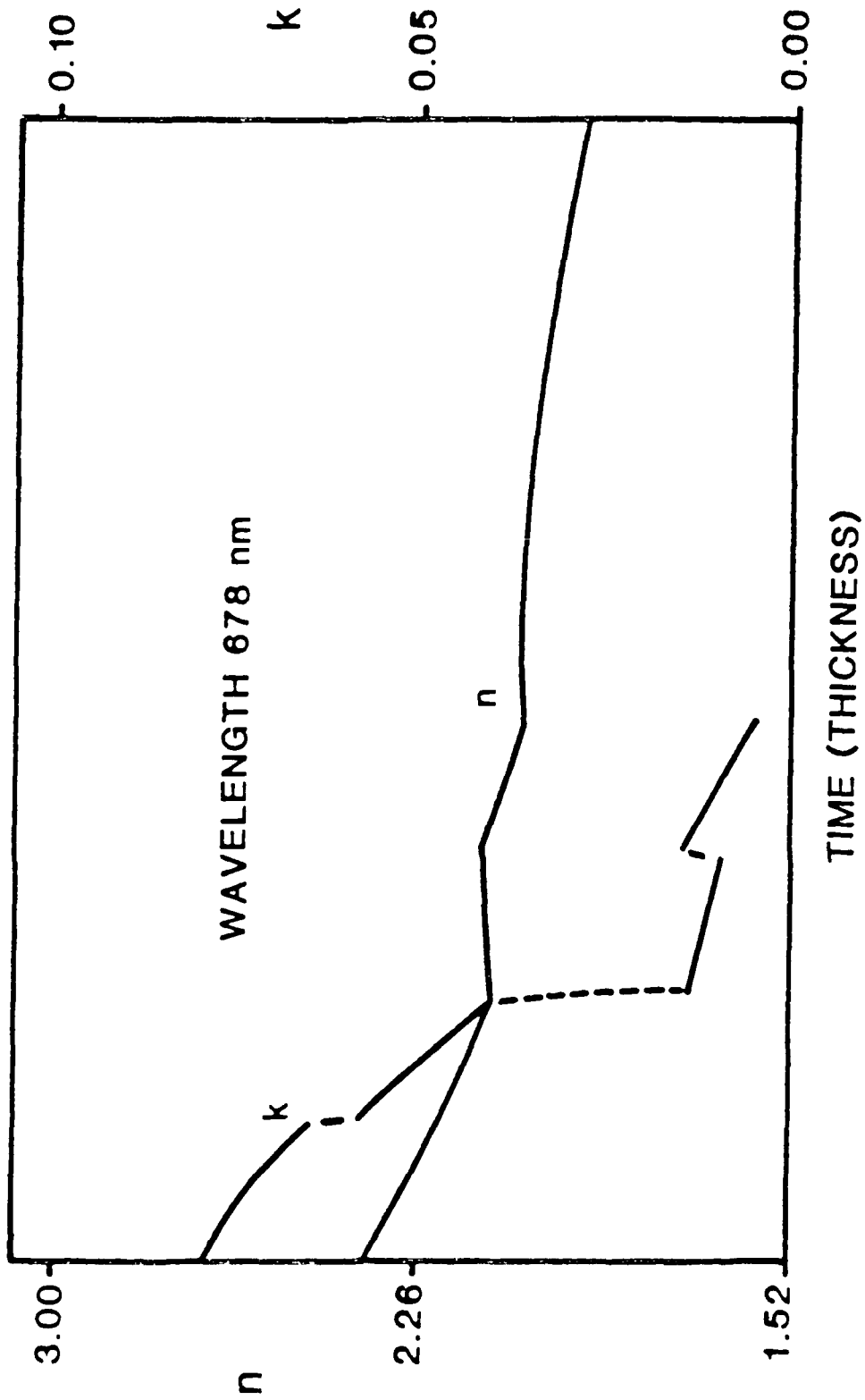


FIG 5. Example of result given by the method when applied to an unstable layer. Titanium dioxide layer deposited in an oxygen deficient atmosphere.

**END**

**FILMED**

4-85

**DTIC**